Appl Phys A (2011) 102: 651–659
DOI 10.1007/s00339-010-6114-1

Applied Physics A
Materials Science & Processing

Liposome micropatterning based on laser-induced forward transfer

Alexandra Palla-Papavlu · Iurie Paraico · James Shaw-Stewart · Valentina Dinca · Tudor Savopol · Eugenia Kovacs · Thomas Lippert · Alexander Wokaun · Maria Dinescu

Received: 12 April 2010 / Accepted: 27 October 2010 / Published online: 16 November 2010
© Springer-Verlag 2010

Abstract The numerous properties of liposomes, i.e., non-toxicity, biodegradability, and their ability to encapsulate different biological active substances in aqueous and lipid phase, make them perfect models of biomembranes. Liposomes made up of phospholipids may be used to study new applications such as cell targeting or, under specific experimental conditions, may be applied in micro and nano-sized biosensors.

This study demonstrates the capability of direct laser printing of liposomes in micron-scale patterns for the realization of biosensors or drug delivery systems.

The transfer experiments were carried out onto ordinary glass substrates, and optical microscopy images reveal that well-defined patterns without splashes can be obtained for a narrow range of laser transfer fluences using 193 nm irradiation and an intermediate triazene polymer. The triazene polymer with different thicknesses was used as sacrificial layer with the purpose of protecting the liposome solution from direct laser irradiation. It was found that the thickness of the sacrificial layer should exceed 150 nm to obtain clean, debris-free patterns. Moreover, the integrity of the liposomes after laser transfer was maintained as demonstrated through fluorescence microscopy. Raman spectroscopy data suggest that the chemical composition of the liposomes does not change for transfer fluences in the range of 40 to 60 mJ/cm^2.

Following these results, one can envision that liposome patterns obtained by LIFT can be ultimately applied for in vitro and in vivo studies.

A. Palla-Papavlu (✉) · V. Dinca · M. Dinescu
National Institute for Lasers, Plasma and Radiation Physics, P.O. Box MG-36, 077125, Bucharest, Romania
e-mail: apalla@nipne.ro

I. Paraico · T. Savopol · E. Kovacs
Department of Biophysics and Cell Biotechnology, "Carol Davila" University of Medicine and Pharmacy, P.O. Box 35-43, Bucharest, Romania

J. Shaw-Stewart
EMPA, Swiss Federal Laboratories for Materials Testing and Research, Laboratory for Functional Polymers, Überlandstrasse 129, 8600 Dübendorf, Switzerland

T. Lippert · A. Wokaun
General Energy Research Department, Paul Scherrer Institute, 5232 Villigen PSI, Switzerland

1 Introduction

Nowadays, a strong research effort is devoted to develop patterning methodologies for the spatially controlled deposition of a wide range of biologically active molecules such as proteins, DNA, and cells onto substrates of different materials (metals, polymers, semiconductors). Patterning of biomolecules, in particular enabling precise positioning of biological active compounds with nano- and micro-scale resolution over large areas, is the main demand in next generation research for analytical and diagnostic applications such as biosensors [1] and microarray chip devices [2].

A large number of techniques for the patterning of biomolecules such as photolithography [3], dip-pen nanolithography [4], micro contact printing [5], electron beam lithography [6], or screen printing [7] have been developed. However, serious limitations exist in the above-mentioned approaches: they are noneconomic due to the usage of large quantities of expensive biological samples, orifice clogging may occur, or contamination issues exist.

As an alternative, laser-based techniques have emerged as a versatile and powerful strategy for engineering biosurfaces with active compounds. In particular, laser-induced

forward transfer (LIFT) was proven to be an appropriate technique which has been successfully used for printing patterns of different materials, including metals [8], oxides [9], and biomolecules, i.e., proteins [10–12], DNA [13, 14], cells [15, 16], and tissue [17].

In LIFT the material is transferred by the laser beam from a transparent support or donor onto an appropriate substrate or receiver. The donor substrate can be previously coated with an intermediate layer, which is called dynamic release layer (DRL) or sacrificial layer. This layer has the purpose to improve the process efficiency and to reduce the risk of damaging the layer to be transferred**.**

In most of the previous studies [10, 14, 18, 19], Ti, Au, Pt, and Cr have been used as sacrificial layers. These metallic sacrificial layers have remarkable advantages, i.e., they are biocompatible, easy to deposit as thin films (i.e., by sputtering), but an important drawback is that debris, i.e., metal fragments, may be present in the transferred material due to incomplete vaporization or cluster condensation.

As an alternative to the metallic layers, UV-sensitive photopolymers, specifically triazene polymers (TP) [20, 21] have emerged as appropriate sacrificial DRL layers. Upon laser irradiation, TP can be efficiently ablated at very low laser fluences, with ablation thresholds in the range of 20–25 mJ/cm^2, and they decompose completely into volatile and gaseous fragments [22].

Doraiswamy et al. [16] and Schiele et al. [23] reported the transfer of biomolecules such as mammalian Chinese hamster ovaries and cells (fibroblasts, myoblasts, neural stem cells, breast cancer cells, and BPAEC) by matrix-assisted pulsed laser evaporation-, direct write (MAPLE DW) using a TP as sacrificial layer [16, 23]. MAPLE-DW is similar to LIFT but requires an additional matrix material.

However, the above-mentioned studies do not offer a thorough investigation of the transfer parameters when applying a polymeric sacrificial layer. These studies are mostly focused on the construction of regular patterns.

The aim of this study is to investigate the controlled positioning of liposomes on solid substrates by understanding how the thickness of the intermediate TP affects the transfer process. The influence of target-substrate distance and laser fluence on the pattern size and shape was examined in addition.

Liposomes are molecular structures composed of lipid bilayers that enclose an aqueous core. The most important properties of liposomes are, for example, nontoxicity, biodegradability, the easy preparation (or production), and stability in solution for a long period of time. These properties make them appealing for applications such as carrier systems of drugs or other functional substances and miniaturized biosensors. The liposomes used in this study are made up of phospholipids and are considered model systems for biomembranes.

Although the liposomes, as prepared for the present study, cannot mimic the functional complexity of an actual cell membrane, they offer the advantage of being cheaper, more stable, and thus representing a perfect cell model system. For further experiments, however, liposomes could be prepared by incorporating biologically active materials such as integral proteins, DNA, or drugs with the purpose of obtaining drug carrier systems.

Following this, one can envision that the liposome patterns obtained by LIFT can ultimately be applied for the transport of drugs and other bioactive capsules to cells or disease-affected tissues or in the development of biosensors.

2 Experimental

2.1 Preparation of the lipid solution

1,2-Dioleoyl-sn-glycero-3-phosphocholine (DOPC) was obtained from Avanti Polar Lipids. All other chemicals were of analytical grade. Deionized water (Milli–Q system; Millipore, Tokio) was used in all experiments. Lipids were dissolved in organic solvents using chloroform or chloroform:methanol 9:1 v:v mixtures to assure a homogeneous mixture of lipids which were stored at −40°C.

The liposomes were prepared based on the "gentle hydration method" [24–26] and by the rotoevaporation method (see below).

2.2 Gentle hydration method

DOPC was dissolved in chloroform to make a total lipid solution of 10 mg/ml. 25 μL of the lipid suspension was placed on a glass coverslip and evaporated by placing under an argon steam, until a thin lipid film is formed. The glass coverslip was placed in a Petri dish and 10 ml of deionized water was added over the dry film.

The temperature of the hydrating medium should be above the gel-liquid crystal transition temperature (T_c) of the lipid. The Petri dish was sealed and incubated at 37°C (above T_c) overnight. During the incubation, the whole lipid film was gradually stripped off the glass surface and formed an almost transparent bulky white cloud floating in the middle of the solution, which contained giant liposomes. Approximately 1 ml of the white cloud was harvested and stored in an Eppendorf tube.

Rhodamine dye was added to the starting lipid mixture at 0.1% by weight for fluorescence imaging of liposome membranes.

2.3 Rotoevaporation method

Giant vesicles were prepared from DOPC dissolved in a chloroform:methanol (9:1 v:v) mixture using the method described in [27].

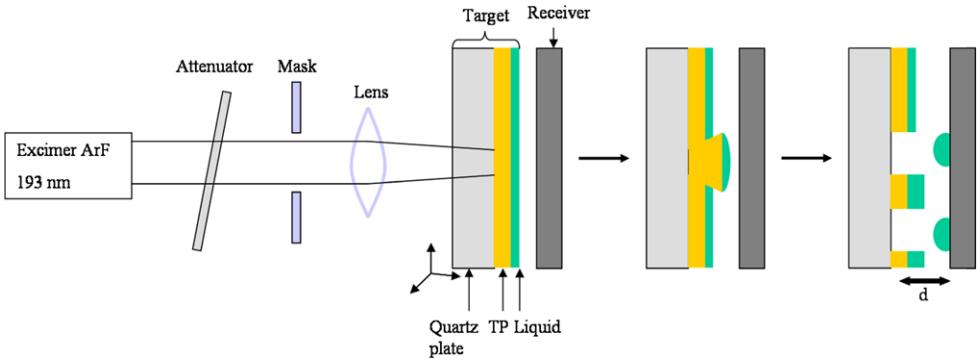

Fig. 1 Experimental setup used for the transfer of liposome solution microdroplets

The organic solvent was removed by rotary evaporation (Heidolph) at 40°C and a rotational speed of 100 rpm, yielding a thin lipid film on the sides of a round bottom flask. The lipid film was thoroughly dried by placing the flask under vacuum for 30 min. 5 ml of double distilled water were added to the round bottom flask over the lipid film maintaining the rotary motion for 15 min, thus obtaining a homogeneous lipid solution. The lipid solution was then transferred in a falcon tube. Rhodamine dye was added to the starting lipid mixture at 0.1% by weight for fluorescence imaging of liposome membranes.

2.4 Targets

The targets were prepared by spin coating the TP (thicknesses 60 nm, 150 nm, and 350 nm) onto fused silica plates (area 5 cm^2, thickness 1 mm) and then drop casting the solution to be transferred. The TP was synthesized as described by Nagel et al. [21] and was then prepared by spin coating from a solution in chlorobenzene and cyclohexanone (1:1, w/w).

The solution to be transferred consisted of a mixture of liposomes, double distilled water and glycerol in concentrations from 10 to 70%. In order to improve the wettability of the TP film, a solution of 0.1–0.3 mg/ml sodium dodecil sulphate (SDS) in double distilled water was added. The liquid film thickness, estimated through the measurement of the film weight, varied from 3 to 10 μm.

2.5 Receiver substrates

The receiver substrates were ordinary glass microscope slides or fused silica plates (5-cm^2 area), which were sterilized prior to the experiments.

2.6 Patterning system

An ArF excimer laser with an emission wavelength of 193 nm (Lambda Physik, 30 ns pulse length, 1 Hz repetition rate) was used to transfer micro droplets of the liposome solution. The scheme of the patterning system is presented in Fig. 1. Briefly, the pulsed UV ArF laser beam was focused through the fused silica plate and onto the TP coated fused silica plate, and microdroplets were transferred from the liquid target (also named "donor") to the receiving surface. The laser energy was varied from 1 to 10 μJ per pulse.

The target and the receiver were placed at an adjustable distance (30 μm–2 mm) on a computer-controlled translation stage while the laser irradiates the target from the backside. The laser beam passed through a mask with an adjustable aperture and was focused by a lens to a spot size of 40 μm to 150 μm in diameter. For each laser pulse, droplets were obtained, which were arranged in a matrix of points.

2.7 Microscopic characterization of the liposomes and liposome patterns

The liposomes prepared by the two methods were investigated by phase contrast microscopy and fluorescence microscopy. The microscopic characterization of the liposomes was performed in a perfusion chamber. The observation chamber was built from a cleaned Corning glass coverslip on top of which a square-shaped spacer made out of double-sided tape was placed. The chamber was filled with the liposome solution. On the top of the spacer, another Corning glass coverslip was placed. In addition, the chamber was precoated with a bovine serum albumin (BSA) 1–2% in double distilled water solution to prevent adhesion of the liposomes.

The phase contrast and fluorescent images were acquired with an Axiovert 200 Microscope coupled to a black and white Carl Zeiss AxioCam MRm camera. The same method was used to characterize the liposome patterns obtained by laser transfer.

Rhodamine stained liposomes were observed by fluorescence microscopy ($\lambda_{ex} = 570$ nm and $\lambda_{ex} = 590$ nm) prior and after laser transfer.

2.8 Raman spectroscopy

Micro-Raman spectroscopy was used to check for any chemical changes in the structure of the liposomes after their

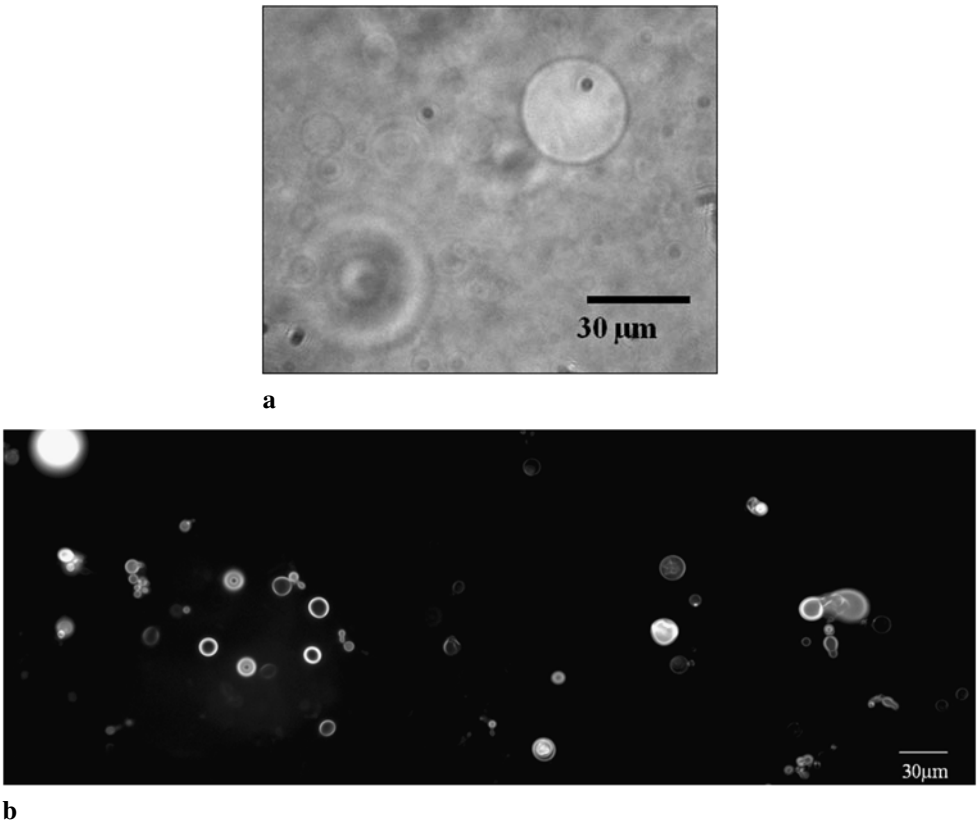

Fig. 2 (**a**) Phase contrast microscopy images of giant liposomes in solution. The images were captured with a 40× objective and (**b**) Fluorescence microscopy images of giant liposomes in solution

transfer. The Raman spectra of the liposomes transferred at different fluences with a 150 nm thick intermediate TP layer were recorded on a Labram HR or Labram confocal Raman microscopy system from Jobin Yvon. The 633 nm line from a HeNe laser was used as an excitation source for the Raman spectra. The laser power at the sample surface was typically 20 mW. For each measurement, the exposure time was 3 min. To improve the signal-to-noise ratio, up to 10 scans were accumulated. The main contribution to the background was water, despite the fact that water is mostly a weak scatterer in the investigated region.

The Raman spectra were collected over the range of 300–3300 cm^{-1}, and all spectra were recorded at room temperature.

3 Results and discussion

3.1 Microscopic observation of the giant liposomes in solution

Giant liposomes with diameters of tens of microns were examined when the liposome suspension is diluted in an external medium, and they can be examined by phase contrast microscopy and fluorescence microscopy (shown in Fig. 2a and b). Most of the giant liposomes appear circular or with distorted circular shape and with peripheries undulating rapidly due to thermal fluctuations. The edges of the liposomes are relatively thick and dark bands due to the difference in the refractive indices of the internal and the external media. Direct observations reveal a weak, but sharp, contrast at the edges of the liposomes, which differs among liposomes. The lowest contrast and fluctuating liposomes are most probably unilamellar (see Fig. 2a) [27].

In addition to giant liposomes, our protocol produced small vesicles and lipid debris.

A fluorescence microscopy image of liposomes in solution is shown in Fig. 2b. The less bright ring-shaped liposomes are settled on the bottom of the perfusion chamber, whereas those which appear brighter are still moving (Brownian motion).

3.2 Influence of the thickness of the DRL layer on the liposome transfer

To avoid laser-induced degradation of the liposomes, a DRL layer is applied. In our approach, the polymeric layer used as DRL is a TP [28]. This TP layer absorbs the laser radiation, decomposes into small, gaseous, molecular fragments and propels the material to be transferred to a receiver support. The use of a TP as DRL has numerous advantages, i.e., (i) the TP has a very low ablation threshold, which means

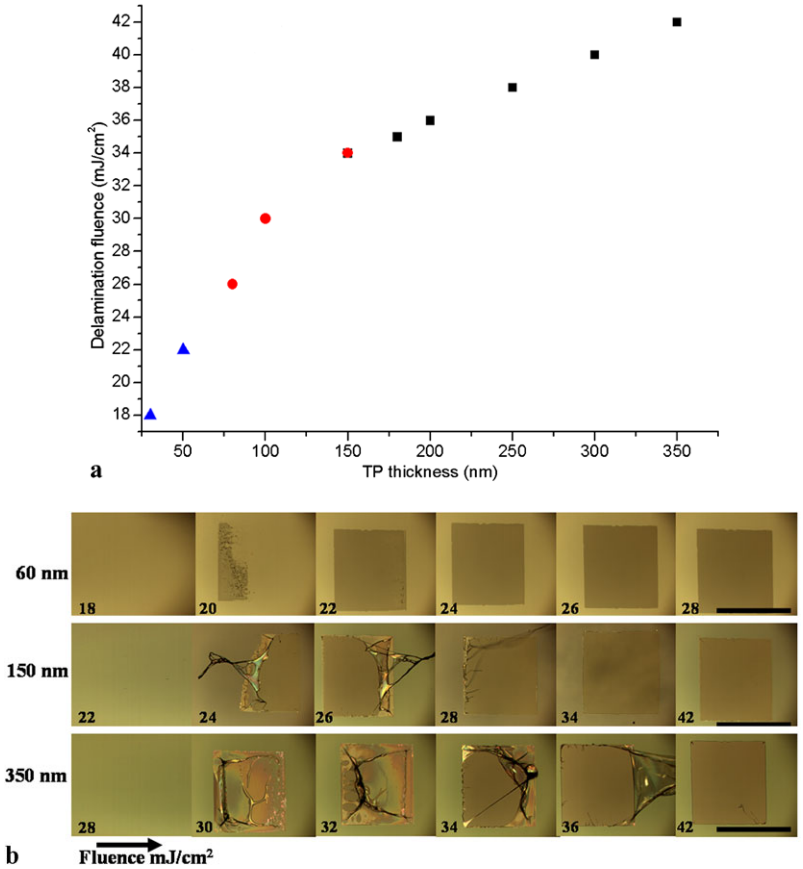

Fig. 3 (**a**) The minimum fluences required for the delamination of a TP layer as a function of the TP thickness. The *red symbols* represent the 60 nm TP layer, the *blue symbols* the 150 nm TP layer, and the *black symbols* the 350 nm TP layer, respectively. (**b**) Optical microscopy images of back-side ablation spots from 60 nm, 150 nm, and 350 nm thick TP films. The fluence increases from *left* to *right*

that the transfer can be achieved with low thermal impact; (ii) no debris is detected; and (iii) a high absorption coefficient at the ArF excimer laser wavelength [22, 29, 30].

In order to obtain debris-free transfer, it is important to find the optimum relation between the thickness of the TP film and the applied laser fluence. Therefore, prior to the liposome solution transfers, back-side ablation experiments were carried out for 60 nm, 150 nm, and 350 nm thick TP layers.

The laser fluence required to achieve a complete removal of the TP layer depends strongly on the film thickness. The minimum laser fluences required for removing a complete TP layer as a function of TP thickness are shown in Fig. 3a, revealing that ablation can, e.g., be achieved with a fluence of ~22 mJ/cm^2 for a 60 nm thick TP layer. Optical microscopy images of back-side ablation spots from 60 nm, 150 nm, and 350 nm thick TP films (shown in Fig. 3b) reveal that for lower fluences, the TP layer is not completely removed, but a slight increase of fluence (e.g., from 20 to 22 mJ/cm^2 in the case of the 60 nm thick film) results in complete delamination. For the 350 nm thick TP layer, more than 42 mJ/cm^2 are needed to achieve complete delamination. For the thicker films (150 and 350 nm), a remaining "skin layer" is observed (see Fig. 3b) for low irradiation fluences, which is still connected to the remaining film. The formation of a skin layer has also been observed for an irradiation wavelength of 308 nm, although for different fluences [31].

After these preliminary experiments, the transfer of liposome solutions with TP films of 60 nm, 150 nm, and 350 nm has been analyzed while the thickness of the liquid layer (3 μm) and the distance between the target and the receiver was kept constant at 400 μm.

It was found that with a TP thickness of 60 nm, no pattern is obtained, and only splashes and irregular droplets are transferred. In this case the TP layer is probably too thin to protect the soft, easily damageable biomolecules. Regular droplets are obtained with TP layers thicker than 150 nm. An optical microscopy image of a printed liposome micro-array obtained with a 350 nm thick TP layer is shown in Fig. 4a. The corresponding fluorescence image of the printed liposome microarray is shown in Fig. 4b. All transferred droplets are regularly arranged with some randomly distributed small droplets around them. The transferred droplets are well defined and compact with no visible changes in the morphology or debris from the TP.

Due to the fact that the fluences applied for the transfer of the liposome solution were lower (i.e., 34 mJ/cm^2) than the fluences needed for the complete vaporization of the 350 nm thick TP layer (approximately 50 mJ/cm^2), it

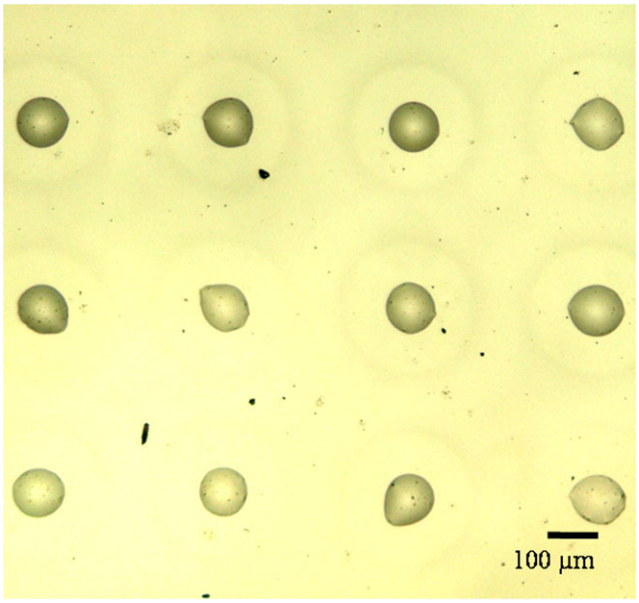

a

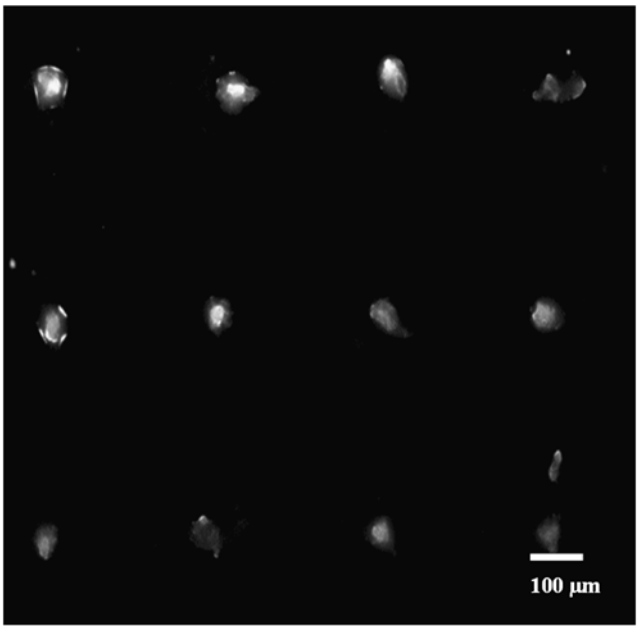

b

Fig. 4 (**a**) Optical microscopy image of a printed liposome micro-array with a 350 nm thick TP layer. (**b**) Fluorescence microscopy image of a printed liposome microarray (corresponding to (**a**)) applying a 350 nm thick TP layer

might be possible that debris from the TP layer appears in the transferred patterns. The data suggest that a 150 nm thick TP layer is sufficient to minimize the damages to the transfer liquid layer and that the fluences necessary to transfer regular droplets must be higher than the fluences needed for the complete vaporization of the TP layer (in this case 35 mJ/cm^2).

Our results agree with previous data [16] and show that it is possible to transfer soft biomaterials without any damage by the ArF laser system despite the fact that the TP was specifically designed for an irradiation wavelength of 308 nm.

3.3 Influence of the laser fluence on the deposits

Previous studies on liquid transfer with a metallic sacrificial layer [32, 33] show that the shape and size of the transferred patterns depend on the laser fluence, but whether this is also valid for the transfer with a TP DRL layer has not yet been established.

Optical micrographs of liposome solution droplets obtained immediately after transfer at different energies per pulse are displayed in Fig. 5a. The laser fluence was varied over a broad range, i.e., from conditions insufficient to detach any material from the target to a high fluences (~35–200 mJ/cm^2), in order to optimize the shape of the transferred droplets without any chemical modifications of the liposomes. For a TP layer with a thickness of 350 nm, the shape of the droplets is well defined in a narrow range of fluences, i.e., between 35 and 60 mJ/cm^2.

The threshold fluence for the transfer of the liposome solution from the irradiated area with a diameter of 80 µm is 35 mJ/cm^2, which is lower than the energy needed for the complete vaporization of the triazene polymer layer with thickness of 350 nm, which occurs at a fluence above 50 mJ/cm^2. No transfer occurs at fluences below 34 mJ/cm^2, while at fluences above 60 mJ/cm^2, splashes surround the spot are observed, and for even higher fluences, the transfer features become irregular.

The target immediately after the transfer is shown in Fig. 5b. The photos reveal that in the range of fluences where regular patterns are obtained, the TP is not completely removed from the substrate.

Moreover, fluorescence microscopy was used to determine whether the integrity of the liposomes was altered after laser transfer. A fluorescence image of a microarray obtained at different laser fluences is presented in Fig. 6. Only at fluences between 40 and 80 mJ/cm^2 the transferred spots exhibit fluorescence corresponding to their density in the target solution. The transferred spots are not surrounded by splashes for fluences of 40 to 60 mJ/cm^2, while for fluences up to 80 mJ/cm^2, random droplets appear on the substrate. Above 80 mJ/cm^2, no fluorescence is detected anymore suggesting that in this case liposome destruction occurred due to high laser fluences.

It can therefore be concluded that the laser fluence is a very important parameter for printing droplets with high resolution, reproducibility, and integrity of the biomolecules.

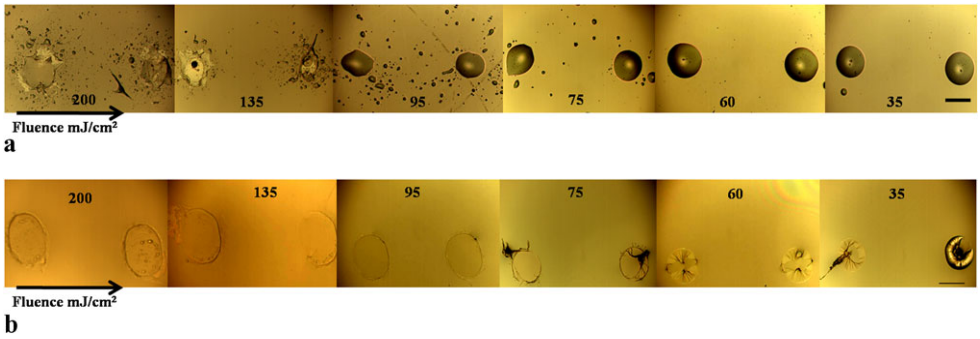

Fig. 5 (**a**) Optical microscopy images of liposome droplets obtained by using different fluences for the transfer and a TP layer of 350 nm thickness. The fluence decreases from *left* to *right*. (**b**) Optical microscopy images of the target after irradiation at different laser fluences with a 350 nm thick TP layer, which corresponds to the transferred droplets in (**a**). The fluences decrease from *left* to *right*

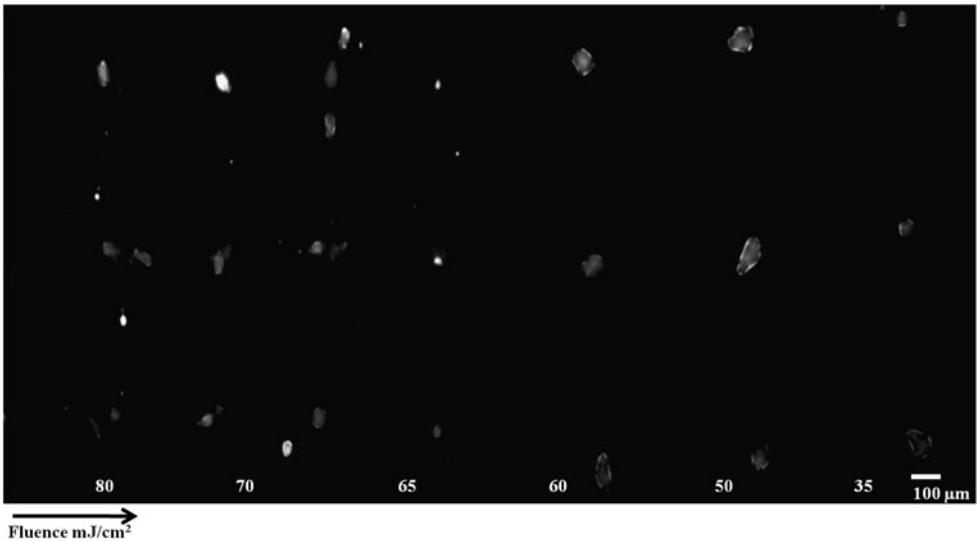

Fig. 6 Fluoresce image of a microarray of liposome solution obtained at different laser fluences. The laser fluences decrease from *left* to *right*

3.4 Influence of target-substrate distance

The influence of the target-substrate distance on the size and shape of the transferred patterns by using the TP as sacrificial layer with different thicknesses was also analyzed. It is very interesting to compare the transfer for the LIFT process with TP as sacrificial layer to Au or Ti layers. What distinguishes the classical Au or Ti thin films from the photosensitive TP layers used as sacrificial layers is the absence of ejected material "debris" after the irradiation process in the case of TP. This behavior is rarely observed with any other materials [34], and metals are detected in the transferred materials which may alter the properties of the biomaterials.

A study on the influence of the target-substrate distance was presented by Dinca et al. in [35], where they studied the transfer of a phosphate buffer saline (PBS) and glycerol solution (50:50 in volume) with a 10 nm thick Au sacrificial layer. The applied laser system was a KrF excimer laser (248 nm, 15 ns pulse length, 1 Hz repetition rate), and the values of the laser fluences were in the range 0.1 to 0.5 J/cm^2. The authors showed that by varying the target-receiver distance from 20 µm to 1 mm no significant changes of the deposited features occur.

In our experiments the model system was a solution of double distilled water and glycerol (50:50 in volume) which was drop cast on top of 150 nm and 350 nm thick TP films. Double distilled water was chosen over PBS because the liposomes used in this study do not require a certain pH for preservation of the native state as the proteins used in [34].

The transfer was performed at a laser fluence of 40 mJ/cm^2, and the droplets were analyzed by optical microscopy. The distance between the target and substrate was varied from 50 µm to 2 mm.

The results show that in the case of TP as sacrificial layer, the size and the shape of the transferred patterns did not change by varying the distance between the target and the substrate. The droplet size dependence as a function of the target-receiver distance for a 150 nm thick TP film is shown in Fig. 7. Similar results are obtained for a 350 nm thick TP layer.

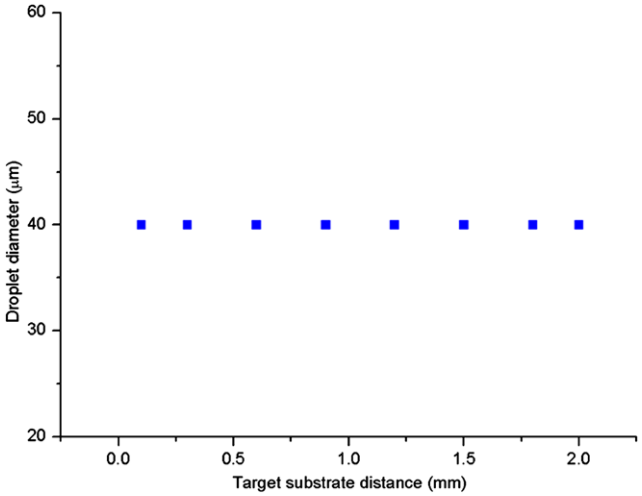

Fig. 7 Dependence of the droplet diameter on the target-receiver distance. The target consisted of glycerol and double distilled water suspension (50:50 in volume) on top of a 150 nm TP film. The applied fluence was 40 mJ/cm^2

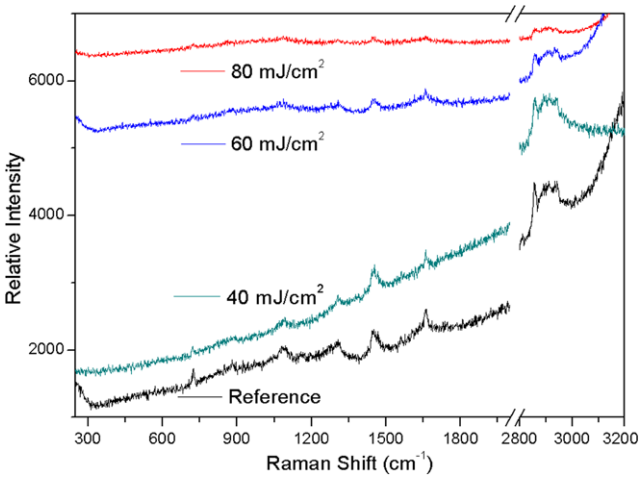

Fig. 8 Raman spectra of the liposome solution after transfer at different laser fluences

On the basis of the results described above, we can conclude that the target-substrate distance is not important in obtaining debris-free and circular-shaped patterns.

3.5 Raman microscopy

Due to the fact that μ-Raman spectroscopy is a noninvasive and nondestructive technique, we used it in our study to investigate the chemical composition of the liposomes after the laser transfer.

The spectrum of lipids is to a large extent due to vibrations in the hydrocarbon chains, but vibrations in the head group region can be used as specific lipid fingerprints.

The μ-Raman reference spectrum (Fig. 8) of the liposomes agrees well with literature data, although it has a lower signal-to-noise ratio than for the reported data [36]. The reason for the low signal was the use of a low laser power in order to minimize the thermal effects on the liposomal membrane at the expense of a slight increase of the background. The assignment of the most important peaks is summarized in Table 1.

Table 1 Vibrational assignment of the major Raman bands of DOPC

Bands [cm^{-1}]	Assignment
1082	C–C stretching
1125	C–C stretching
1264	cis C = C
1296	CH_2 twist
1445	CH_2 bend
1655	cis C = C
2800–3100	CH stretching

The two regimes of the spectrum where differences in lipid structure are most notable come from C–C backbone vibrations (1050–1150 cm^{-1}) and the C–H stretching modes (2800–3200 cm^{-1}). The bands ~2973 cm^{-1} (shoulder) and 3023 cm^{-1} are attributed to the asymmetric and symmetric CH_3 stretching modes of the choline headgroup [35].

Raman spectra taken of transferred liposomes using different laser fluences (see Fig. 8) shows a clear tendency: the intensity of characteristic Raman peaks decreases with increasing laser fluence. Still, the Raman spectra taken at fluences below 60 mJ/cm^2 can be identified as liposome, while for fluences above this value, chemical modification of the liposomes take place upon laser transfer. In addition, there are no indications of triazene being present in the transferred liposomes.

The Raman analysis of the lipids suggests that the liposomal membranes are not damaged for laser fluences below 60 mJ/cm^2 and that the TP does probably not contaminate the lipids.

4 Conclusions

We show in this work that the application of a laser processing technique, i.e., LIFT, is a promising approach for printing liposome solutions for biosensor or drug delivery systems. The transfer process of liposome solutions was optimized by applying intermediate DRL layers with different thicknesses. It was found that only for TP layer thicker than 150 nm, a clean transfer can be obtained. Optical microscopy images reveal that well-defined patterns with clearly circular shape can be obtained for laser transfer fluences in the range of 40 to 60 mJ/cm^2 using 193 nm irradiation. The target-substrate distance is a parameter that does not influence the morphology of the obtained micropatterns. Moreover, the Raman spectroscopy data suggest

that the chemical composition of the liposomes does not change for transfer fluences from 40 to 60 mJ/cm^2.

The fact that liposome arrays can be produced cost- and time-effectively with a minimum sample volume required suggests that LIFT is a promising technique for transferring liposome solutions, which can therefore be applied for in vitro and in vivo applications.

Acknowledgements Financial support from the NATO SFP project 982671, EU FP7 program eLIFT, and National Project IDEI no. 1197/2008 are gratefully acknowledged. The authors acknowledge Matthias Nagel for the synthesis of the triazene polymer, Sebastian Heiroth for help with the patterning setup, and Kurt Ballmer for the fluorescence microscopy images.

References

1. Y. Cui, Q.Q. Wei, H.K. Park, C.M. Lieber, Science **293**, 1289–1292 (2001)
2. I. Zergiotti, A. Karaiskou, D.G. Papazoglou, C. Fotakis, M. Kaspsetaki, D. Kafetzoupoulous, Appl. Phys. Lett. **86**, 163902 (2005)
3. B. Schmidt, V. Almeida, C. Manolatou, S. Preble, M. Lipson, Appl. Phys. Lett. **85**, 4854 (2004)
4. K.-B. Lee, S.-J. Park, C.A. Mirkin, J.A. Smith, M. Mrksich, Science **295**, 1702 (2002)
5. D.J. Graber, T.J. Zieziulewicz, D.A. Lawrence, W. Shain, J.N. Turner, Langmuir **19**, 5431 (2003)
6. G.J. Zhang, T. Tanii, T. Zako, T. Hosaka, T. Miyake, Y. Kanari, T. Funatsu, I. Ohdomari, Small **1**, 833 (2005)
7. T. Schuler, T. Asmus, W. Fritzsche, R. Moller, Biosens. Bioelectron. **24**, 2077 (2009)
8. I. Zergioti, S. Mailis, N.A. Vainos, P. Papakonstantinou, C. Kalpouzos, C.P. Grigoropoulous, C. Fotakis, Appl. Phys. A **66**, 579–582 (1998)
9. A. Klini, A. Mourka, V. Dinca, C. Fotakis, F. Claeyssens, Appl. Phys. A, Mater. Sci. Process. **87**(1), 17–22 (2007)
10. V. Dinca, A. Ranella, M. Farsari, D. Kafetzopoulous, M. Dinescu, A. Popescu, C. Fotakis, Biomed. Microdevices **10**, 719–725 (2008)
11. J.M. Fernandez-Pradas, M. Colina, P. Serra, J. Domınguez, J.L. Morenza, Thin Solid Films **27**, 453–454C (2004)
12. D.B. Chrisey, Science **289**, 879 (2000)
13. A. Karaiskou, I. Zergioti, C. Fotakis, M. Kapsetaki, D. Kafetzopoulos, Appl. Surf. Sci. **245**, 208–209 (2003)
14. P. Serra, M. Colina, J.M. Fernandez-Paras, L. Sevilla, J.L. Morenza, Appl. Phys. Lett. **85**, 1639–1641 (2004)
15. B.R. Ringeisen et al., Am. Biotechnol. Lab. **19**, 42 (2001)
16. A. Doraiswamy et al., Appl. Surf. Sci. **252**, 4743–4747 (2006)
17. D.B. Chrisey, A. Pique, R.A. McGill, J.S. Horwitz, B.R. Ringeisen, D.M. Bubb, P.K. Wu, Chem. Rev. **103**, 553 (2003)
18. V. Dinca, E. Kasotakis, J. Catherine, A. Mourka, A. Mitraki, A. Popescu, M. Dinescu, M. Farsari, C. Fotakis, Appl. Surf. Sci. **254**, 1160–1163 (2007)
19. C. Boutopoulous, V. Tsouti, D. Goustouridis, S. Chatzandroulis, I. Zergiotti, Appl. Phys. Lett. **93**, 191109 (2008)
20. R. Fardel, M. Nagel, F. Nuesch, T.K. Lippert, A. Wokaun, Appl. Surf. Sci. **254**, 1322–1326 (2007)
21. M. Nagel, R. Fardel, P. Feurer, M. Häberli, F. Nüesch, T.K. Lippert, A. Wokaun, Appl. Phys. A **92**, 781–789 (2008)
22. T. Lippert, Adv. Polym. Sci. **168**, 51–246 (2004)
23. N. Schiele, R.A. Koppes, D.T. Corr, K.S. Ellison, D.M. Thompson, L.A. Ligon, T.K.M. Lippert, D.B. Chrisey, Appl. Surf. Sci. **255**, 5444–5447 (2009)
24. J.P. Reeves, R.M. Dowben, J. Membr. Biol. **3**, 123–141 (1970)
25. P. Mueller, T.F. Chien, B. Rudy, Biophys. J. **44**, 375–381 (1983)
26. D. Needham, E. Evans, Biochemistry **27**, 4668–4673 (1988)
27. K. Akashi, H. Miyata, H. Itoh, K. Kinosita Jr., Biophys. J. **71**, 3242–3250 (1996)
28. M. Nagel, R. Hany, T. Lippert, M. Molberg, F.A. Nüesch, D. Rentsch, Macromol. Chem. Phys. **208**, 277–286 (2007)
29. T. Lippert, L.S. Bennett, T. Nakamura, H. Niino, A. Ouchi, A. Yabe, Appl. Phys. A **63**, 257 (1996)
30. T. Lippert, Plasma Process. Polym. 525 (2005)
31. R. Fardel, M. Nagel, F. Nuesch, T.K. Lippert, A. Wokaun, Appl. Surf. Sci. **254**, 1332–1337 (2007)
32. V. Dinca, A. Ranella, A. Popescu, M. Dinescu, M. Farsari, C. Fotakis, Appl. Surf. Sci. **254**, 1164–1168 (2007)
33. P. Serra, J.M. Fernandez-Pradas, M. Colina, M. Duocastella, J. Dominguez, J.L. Morenza, J. Laser Micro/Nanoeng. **3**, 236 (2006)
34. L. Rapp, C. Cibert, A.P. Alloncle, P. Delaporte, Appl. Surf. Sci. **255**(10), 5439–5443 (2009)
35. V. Dinca, M. Farsari, D. Kafetzopoulos, A. Popescu, M. Dinescu, C. Fotakis, Thin Solid Films **516**, 6504–6511 (2008)
36. D.P. Cherney, J.C. Conboy, J.M. Harris, Anal. Chem. **75**(23), 6621–6628 (2003)